COMMUNICATION-EFFICIENT AND DRIFT-ROBUST FEDERATED LEARNING VIA ELASTIC NET

Anonymous authors
Paper under double-blind review

ABSTRACT

Federated learning (FL) is a distributed method to train a global model over a set of local clients while keeping data localized. It reduces the risks of privacy and security but faces important challenges including expensive communication costs and client drift issues. To address these issues, we propose FedElasticNet, a communication-efficient and drift-robust FL framework leveraging the elastic net. It repurposes two types of the elastic net regularizers (i.e., ℓ_1 and ℓ_2 penalties on the local model updates): (1) the ℓ_1-norm regularizer sparsifies the local updates to reduce the communication costs and (2) the ℓ_2-norm regularizer resolves the client drift problem by limiting the impact of drifting local updates due to data heterogeneity. FedElasticNet is a general framework for FL; hence, without additional costs, it can be integrated into prior FL techniques, e.g., FedAvg, FedProx, SCAFFOLD, and FedDyn. We show that our framework effectively resolves the communication cost and client drift problems simultaneously.

1 INTRODUCTION

Federated learning (FL) is a collaborative method that allows many clients to contribute individually to training a global model by sharing local models rather than private data. Each client has a local training dataset, which it does not want to share with the global server. Instead, each client computes an update to the current global model maintained by the server, and only this update is communicated. FL significantly reduces the risks of privacy and security (McMahan et al., 2017; Li et al., 2020a), but it faces crucial challenges that make the federated settings distinct from other classical problems (Li et al., 2020a) such as expensive communication costs and client drift problems due to heterogeneous local training datasets and heterogeneous systems (McMahan et al., 2017; Li et al., 2020a; Konečný et al., 2016a;b).

Communicating models is a critical bottleneck in FL, in particular when the federated network comprises a massive number of devices (Bonawitz et al., 2019; Li et al., 2020a; Konečný et al., 2016b). In such a scenario, communication in the federated network may take a longer time than that of local computation by many orders of magnitude because of limited communication bandwidth and device power (Li et al., 2020a). To reduce such communication cost, several strategies have been proposed (Konečný et al., 2016b; Li et al., 2020a). In particular, Konečný et al. (2016b) proposed several methods to form structured local updates and approximate them, e.g., subsampling and quantization. Reisizadeh et al. (2020); Xu et al. (2020) also proposed an efficient quantization method for FL to reduce the communication cost.

Also, in general, as the datasets that local clients own are heterogeneous, trained models on each local data are *inconsistent* with the global model that minimizes the global empirical loss (Karimireddy et al., 2020; Malinovskiy et al., 2020; Acar et al., 2021). This issue is referred to as the *client drift* problem. In order to resolve the client drift problem, FedProx (Li et al., 2020b) added a proximal term to a local objective function and regulated local model updates. Karimireddy et al. (2020) proposed SCAFFOLD algorithm that transfers both model updates and control variates to resolve the client drift problem. FedDyn (Acar et al., 2021) dynamically regularizes local objective functions to resolve the client drift problem.

Unlike most prior works focusing on either the communication cost problem or the client drift problem, we propose a technique that effectively resolves the communication cost and client drift problems simultaneously.

	FedAvg	FedProx	SCAFFOLD	FedDyn	**FedElasticNet**
Communication efficiency	△	△	×	△	○
Robustness to heterogeneous data	×	△	○	○	○

Table 1: Comparison of prior methods and the proposed FedElasticNet.

Contributions In this paper, we propose FedElasticNet, a new framework for communication-efficient and drift-robust FL. It repurposes the ℓ_1-norm and ℓ_2-norm regularizers of the elastic net (Zou & Hastie, 2005), by which it successfully improves (i) communication efficiency by adopting the ℓ_1-norm regularizer and (ii) robustness to heterogeneous local datasets by adopting the ℓ_2-norm regularizer.

FedElasticNet is a general framework; hence, it can be integrated with prior FL algorithms such as FedAvg (McMahan et al., 2017), FedProx (Li et al., 2020b), SCAFFOLD (Karimireddy et al., 2020), and FedDyn (Acar et al., 2021) so as to resolve the client drift problem as well as the communication cost problem. Further, it incurs no additional costs in training. Empirically, we show that FedElasticNet enhances communication efficiency while maintaining the classification accuracy even for heterogeneous datasets, i.e., the client drift problem is resolved. Theoretically, we characterize the impact of the regularizer terms. Table 1 compares the prior methods and the proposed FedElasticNet if integrated with FedDyn (Algorithm 3).

2 Related Work

To address the communication cost and client drift problems, numerous approaches were proposed. Here, we describe closely related works that we consider baseline methods. The comprehensive reviews can be found in Kairouz et al. (2021); Li et al. (2020a).

FedAvg (McMahan et al., 2017) is one of the most commonly used methods. FedAvg tackles the communication bottleneck issue by performing multiple local updates before communicating to the server. It works well for homogeneous datasets across clients (McMahan et al., 2017; Karimireddy et al., 2020), but it is known that FedAvg may diverge when local datasets are heterogeneous (Zhao et al., 2018; Li et al., 2020a).

FedProx (Li et al., 2020b) addressed the data heterogeneity problem. FedProx introduces an ℓ_2-norm regularizer to the local objective functions to penalize local updates that are far from the server's model and thus to limit the impact of variable local updates (Li et al., 2020b). Although FedProx is more robust to heterogeneous datasets than FedAvg, the regularizer does not result in aligning the global and local stationary points (Acar et al., 2021). Also, we note that FedProx does not improve communication efficiency compared to that of FedAvg.

SCAFFOLD (Karimireddy et al., 2020) defined *client drift* that the model created by aggregating local models and the optimal global model is inconsistent because of heterogeneous local datasets. SCAFFOLD communicates the trained local models and the clients' control variates so as to resolve the client drift problem. Hence, SCAFFOLD requires twice the communication cost compared to other FL algorithms.

FedDyn (Acar et al., 2021) dynamically updates its local regularizers at each round to ensure that the local clients' optima are asymptotically consistent with stationary points of the global empirical loss. Unlike SCAFFOLD, FedDyn resolves the client drift problem without incurring additional communication costs. However, FedDyn's communication cost is not improved compared to FedAvg and FedProx.

Zou & Hastie (2005) proposed the elastic net to encourage the grouping effect, in other words, to encourage strongly correlated covariates to be in or out of the model description together (Hu et al., 2018). Initially, the elastic net was proposed to overcome the limitations of Lasso (Tibshirani, 1996) imposing an ℓ_1-norm penalty on the model parameters. For instance of a linear least square problem, the objective of Lasso is to solve

$$\min_{\theta} \|y - \mathbf{X}\theta\|_2^2 + \lambda_1 \|\theta\|_1 , \tag{1}$$

where y is the outcome and $\mathbf{X}$ is the covariate matrix. Lasso performs both variable selection and regularization to enhance the prediction accuracy and interpretability of the resulting model. However, it has some limitations, especially for high-dimensional models. If a group of variables is highly correlated, then Lasso tends to select only one variable from the group and does not care which one is selected (Zou & Hastie, 2005). The elastic net overcomes these limitations by adding an ℓ_2-norm penalty. The objective of the elastic net is to solve

$$\min_{\theta} \|y - \mathbf{X}\theta\|_2^2 + \frac{\lambda_2}{2} \|\theta\|_2^2 + \lambda_1 \|\theta\|_1 . \tag{2}$$

The elastic net simultaneously enables automatic variable selection and continuous shrinkage by the ℓ_1-norm regularizer and enables to select groups of correlated variables by its ℓ_2-norm regularizer (Zou & Hastie, 2005). We will leverage the elastic net approach to resolve the critical problems of FL: expensive communication cost and client drift problems.

3 Proposed Method: FedElasticNet

We assume that m local clients communicate with the global server. For the kth client (where $k \in [m]$) participating in each training round, we assume that a training data feature $x \in \mathcal{X}$ and its corresponding label $y \in \mathcal{Y}$ are drawn IID from a device-indexed joint distribution, i.e., $(x, y) \sim P_k$ (Acar et al., 2021). The objective is to find

$$\arg\min_{\theta \in \mathbb{R}^d} \left[\mathcal{R}(\theta) := \frac{1}{m} \sum_{k \in [m]} L_k(\theta) \right], \tag{3}$$

where $L_k(\theta) = \mathbb{E}_{x \sim P_k}\left[l_k(\theta; (x, y)) \right]$ is the local risk of the kth clients over possibly heterogeneous data distributions P_k. Also, θ represents the model parameters and $l_k(\cdot)$ is a loss function such as cross entropy (Acar et al., 2021).

FedElasticNet The proposed method (FedElasticNet) leverages the elastic net approach to resolve the communication cost and client drift problems. We introduce the ℓ_1-norm and ℓ_2-norm penalties on the local updates: In each round $t \in [T]$, the kth local client attempts to find θ_k^t by solving the following optimization problem:

$$\theta_k^t = \arg\min_{\theta} L_k(\theta) + \frac{\lambda_2}{2} \left\|\theta - \theta^{t-1}\right\|_2^2 + \lambda_1 \left\|\theta - \theta^{t-1}\right\|_1 , \tag{4}$$

where θ^{t-1} denotes the global model received from the server. Then, it transmits the difference $\Delta_k^t = \theta_k^t - \theta^{t-1}$ to the server.

Inspired by the elastic net, we introduce two types of regularizers for local objective functions; however, each of them works in a different way so as to resolve each of the two FL problems: the communication cost and client drift problems. First, the ℓ_2-norm regularizer resolves the client drift problem by limiting the impact of variable local updates as in FedProx (Li et al., 2020b). FedDyn (Acar et al., 2021) also adopts the ℓ_2-norm regularizer to control the client drift.

Second, the ℓ_1-norm regularizer attempts to sparsify the local updates $\Delta_k^t = \theta_k^t - \theta^{t-1}$. We consider two ways of measuring communication cost: One is the number of nonzero elements in Δ_k^t (Yoon et al., 2021; Jeong et al., 2021), which the ℓ_1-norm sparsifies. The other is the (Shannon) entropy since it is the theoretical lower bound on the data compression (Cover & Thomas, 2006). We demonstrate that the ℓ_1-norm penalty on the local updates can effectively reduce the number of nonzero elements as well as the entropy in Section 4. To boost sparseness of $\Delta_k^t = \theta_k^t - \theta^{t-1}$, we sent $\Delta_k^t(i) = 0$ if $|\Delta_k^t(i)| \leq \epsilon$ where $\Delta_k^t(i)$ denotes the ith element of Δ_k^t. The parameter ϵ is chosen in a range that does not affect classification accuracy.

Our FedElasticNet approach can be integrated into existing FL algorithms such as FedAvg (McMahan et al., 2017), SCAFFOLD (Karimireddy et al., 2020), and FedDyn (Acar et al., 2021) without additional costs, which will be described in the following subsections.

Algorithm 1 FedElasticNet for FedAvg & FedProx

```
Input: $T, \theta^0, \lambda_1 > 0, \lambda_2 > 0$
1: for each round $t = 1, 2, ..., T$ do
2:     Sample devices $\mathcal{P}_t \subseteq [m]$ and transmit $\theta^{t-1}$ to each selected local client
3:     for each local client $k \in \mathcal{P}_t$ do in parallel
4:         Set $\theta_k^t = \arg\min_{\theta} L_k(\theta) + \frac{\lambda_2}{2} \left\| \theta - \theta^{t-1} \right\|_2^2 + \lambda_1 \left\| \theta - \theta^{t-1} \right\|_1$
5:         Transmit $\Delta_k^t = \theta_k^t - \theta^{t-1}$ to the global server
6:     end for
7:     Set $\theta^t = \theta^{t-1} + \sum_{k \in \mathcal{P}_t} \frac{n_k}{n} \Delta_k$
8: end for
```

Algorithm 2 FedElasticNet for SCAFFOLD

```
Input: $T, \theta^0, \lambda_1 > 0, \lambda_2 > 0$, global step size $\eta_g$, and local step size $\eta_l$.
for each round $t = 1, 2, ..., T$ do
    Sample devices $\mathcal{P}_t \subseteq [m]$ and transmit $\theta^{t-1}$ and $c^{t-1}$ to each selected device
    for each device $k \in \mathcal{P}_t$ do in parallel
        Initialize local model $\theta_k^t = \theta^{t-1}$
        for $b = 1, \ldots, B$ do
            Compute mini-batch gradient $\nabla L_k(\theta_k^t)$
            $\theta_k^t \leftarrow \theta_k^t - \eta_l \left( \nabla L_k(\theta_k^t) - c_k^{t-1} + c^{t-1} + \lambda_2(\theta_k^t - \theta^{t-1}) + \lambda_1 \text{sign}(\theta_k^t - \theta^{t-1}) \right)$
        end for
        Set $c_k^t = c_k^{t-1} - c^{t-1} + \frac{1}{B\eta_l}(\theta^{t-1} - \theta_k^t)$
        Transmit $\Delta_k^t = \theta_k^t - \theta^{t-1}$ and $\Delta c_k = c_k^t - c_k^{t-1}$ to the global server
    end for
    Set $\theta^t = \theta^{t-1} + \frac{\eta_g}{|\mathcal{P}_t|} \sum_{k \in \mathcal{P}_t} \Delta_k$
    Set $c^t = c^{t-1} + \frac{1}{m} \sum_{k \in \mathcal{P}_t} \Delta c_k$
end for
```

3.1 FedElasticNet for FedAvg & FedProx (FedAvg & FedProx + Elastic Net)

Our FedElasticNet can be applied to FedAvg (McMahan et al., 2017) by adding two regularizers on the local updates, which resolves the client drift problem and the communication cost problem. As shown in Algorithm 1, the local client minimizes the local objective function (4). In Step 7, n and n_k denote the total numbers of data points of all clients and the data points of the kth client, respectively.

It is worth mentioning that FedProx uses the ℓ_2-norm regularizer to address the data and system heterogeneities (Li et al., 2020b). By adding the ℓ_1-norm regularizer, we can sparsify the local updates of FedProx and thus effectively reduce the communication cost. Notice that Algorithm 1 can be viewed as the integration of FedProx and FedElasticNet.

3.2 FedElasticNet for SCAFFOLD (SCAFFOLD + Elastic Net)

In SCAFFOLD, each client computes the following mini-batch gradient $\nabla L_k(\theta_k^t)$ and control variate c_k^t (Karimireddy et al., 2020):

$$\theta_k^t \leftarrow \theta_k^t - \eta_l \left(\nabla L_k \left(\theta_k^t \right) - c_k^{t-1} + c^{t-1} \right), \tag{5}$$

$$c_k^t \leftarrow c_k^{t-1} - c^{t-1} + \frac{1}{B\eta_l}(\theta^{t-1} - \theta_k^t), \tag{6}$$

where η_l is the local step size and B is the number of mini-batches at each round. This control variate makes the local parameters θ_k^t updated in the direction of the global optimum rather than each local optimum, which effectively resolves the client drift problem. However, SCAFFOLD incurs twice much communication cost since it should communicate the local update $\Delta_k^t = \theta_k^t - \theta^{t-1}$ and the control variate $\Delta c_k = c_k^t - c_k^{t-1}$, which are of the same dimension.

In order to reduce the communication cost of SCAFFOLD, we apply our FedElasticNet framework. In the proposed algorithm (see Algorithm 2), each local client computes the following mini-batch gradient instead of (5):

$$\theta_k^t \leftarrow \theta_k^t - \eta_l \left(\nabla L_k \left(\theta_k^t\right) - c_k^{t-1} + c^{t-1} + \lambda_2(\theta_k^t - \theta^{t-1}) + \lambda_1 \mathrm{sign}(\theta_k^t - \theta^{t-1})\right), \tag{7}$$

where $\lambda_1 \mathrm{sign}(\theta_k^t - \theta^{t-1})$ corresponds to the gradient of ℓ_1-norm regularizer $\lambda_1 \|\theta_k^t - \theta^{t-1}\|_1$. This ℓ_1-norm regularizer sparsifies the local update $\Delta_k^t = \theta_k^t - \theta^{t-1}$; hence, reduces the communication cost. Since the control variate already addresses the client drift problem, we can remove the ℓ_2-norm regularizer or set λ_2 as a small value.

3.3 FedElasticNet for FedDyn (FedDyn + Elastic Net)

In FedDyn, each local client optimizes the following local objective, which is the sum of its empirical loss and a penalized risk function:

$$\theta_k^t = \arg\min_{\theta} L_k(\theta) - \langle \nabla L_k(\theta_k^{t-1}), \theta \rangle + \frac{\lambda_2}{2} \left\|\theta - \theta^{t-1}\right\|_2^2, \tag{8}$$

where the penalized risk is dynamically updated so as to satisfy the following first-order condition for local optima:

$$\nabla L_k(\theta_k^t) - \nabla L_k(\theta_k^{t-1}) + \lambda_2(\theta_k^t - \theta^{t-1}) = 0. \tag{9}$$

This first-order condition shows that the stationary points of the local objective function are consistent with the server model (Acar et al., 2021). That is, the client drift is resolved. However, FedDyn makes no difference from FedAvg and FedProx in communication costs.

By integrating FedElasticNet and FedDyn, we can effectively reduce the communication cost of FedDyn as well. In the proposed method (i.e., FedElasticNet for FedDyn), each local client optimizes the following local empirical objective:

$$\theta_k^t = \arg\min_{\theta} L_k(\theta) - \langle \nabla L_k(\theta_k^{t-1}), \theta \rangle + \frac{\lambda_2}{2} \left\|\theta - \theta^{t-1}\right\|_2^2 + \lambda_1 \left\|\theta - \theta^{t-1}\right\|_1, \tag{10}$$

which is the sum of (8) and the additional ℓ_1-norm penalty on the local updates. The corresponding first-order condition is given by

$$\nabla L_k(\theta_k^t) - \nabla L_k(\theta_k^{t-1}) + \lambda_2(\theta_k^t - \theta^{t-1}) + \lambda_1 \mathrm{sign}(\theta_k^t - \theta^{t-1}) = 0. \tag{11}$$

Notice that the stationary points of the local objective function are consistent with the server model as in (9). If $\theta_k^t \neq \theta^{t-1}$ (i.e., $\mathrm{sign}(\theta_k^t - \theta^{t-1}) = \pm 1$), then the first-order condition is

$$\nabla L_k(\theta_k^t) - \nabla L_k(\theta_k^{t-1}) + \lambda_2(\theta_k^t - \theta^{t-1}) = \pm\lambda_1, \tag{12}$$

where λ_1 is a vectorized one. Our empirical results show that the optimized hyperparameter is $\lambda_1 = 10^{-4}$ or 10^{-6} and the impact of $\pm\lambda_1$ in (12) would be negligible. Hence, the proposed FedElasticNet for FedDyn resolves the client drift problem. Further, the local update $\Delta_k^t = \theta_k^t - \theta^{t-1}$ is sparse due to the ℓ_1-norm regularizer, which effectively reduces the communication cost at the same time. The detailed algorithm is described in Algorithm 3.

Algorithm 3 FedElasticNet for FedDyn

```
Input: $T, \theta^0, \lambda_1 > 0, \lambda_2 > 0, h^0 = 0, \nabla L_k\left(\theta_k^0\right) = 0$.
for each round $t = 1, 2, ..., T$ do
    Sample devices $\mathcal{P}_t \subseteq [m]$ and transmit $\theta^{t-1}$ to each selected device
    for each device $k \in \mathcal{P}_t$ do in parallel
        Set $\theta_k^t = \arg\min_{\theta} L_k(\theta) - \left\langle \nabla L_k(\theta_k^{t-1}), \theta \right\rangle + \frac{\lambda_2}{2} \left\|\theta - \theta^{t-1}\right\|_2^2 + \lambda_1 \left\|\theta - \theta^{t-1}\right\|_1$
        Set $\nabla L_k(\theta_k^t) = \nabla L_k\left(\theta_k^{t-1}\right) - \lambda_2\left(\theta_k^t - \theta^{t-1}\right) - \lambda_1 \mathrm{sign}\left(\theta_k^t - \theta^{t-1}\right)$
        Transmit $\Delta_k^t = \theta_k^t - \theta^{t-1}$ to the global server
    end for
    for each device $k \notin \mathcal{P}_t$ do in parallel
        Set $\theta_k^t = \theta_k^{t-1}$ and $\nabla L_k(\theta_k^t) = \nabla L_k\left(\theta_k^{t-1}\right)$
    end for
    Set $h^t = h^{t-1} - \frac{\lambda_2}{m} \sum_{k \in \mathcal{P}_t} \left(\theta_k^t - \theta^{t-1}\right) - \frac{\lambda_1}{m} \sum_{k \in \mathcal{P}_t} \mathrm{sign}(\theta_k^t - \theta^{t-1})$
    Set $\theta^t = \frac{1}{|\mathcal{P}_t|} \sum_{k \in \mathcal{P}_t} \theta_k^t - \frac{1}{\lambda_2} h^t$
end for
```

Convergence Analysis We provide a convergence analysis on FedElasticNet for FedDyn (Algorithm 3).

Theorem 3.1. *Assume that the clients are uniformly randomly selected at each round and the local loss functions are convex and β-smooth. Then Algorithm 3 satisfies the following inequality:*

$$\begin{aligned}\mathbb{E}\left[\mathcal{R}\left(\frac{1}{T}\sum_{t=0}^{T-1}\gamma^t\right)-\mathcal{R}(\theta_*)\right] &\leq \frac{1}{T}\frac{1}{\kappa_0}(\mathbb{E}\|\gamma^0-\theta_*\|_2^2+\kappa C_0)+\frac{\kappa'}{\kappa_0}\cdot\lambda_1^2 d \\ &\quad -\frac{1}{T}\frac{2\lambda_1}{\lambda_2}\sum_{t=1}^{T}\left\langle\gamma^{t-1}-\theta_*,\frac{1}{m}\sum_{k\in[m]}\mathbb{E}[\mathrm{sign}(\tilde{\theta}_k^t-\theta^{t-1})]\right\rangle, \qquad (13)\end{aligned}$$

where $\theta_* = \arg\min_\theta \mathcal{R}(\theta)$, $P = |\mathcal{P}_t|$, $\gamma^t = \frac{1}{P}\sum_{\mathcal{P}_t}\theta_k^t$, $d = \dim(\theta)$, $\kappa = \frac{10m}{P}\frac{1}{\lambda_2}\frac{\lambda_2+\beta}{\lambda_2^2-25\beta^2}$, $\kappa_0 = \frac{2}{\lambda_2}\frac{\lambda_2^2-25\lambda_2\beta-50\beta^2}{\lambda_2^2-25\beta^2}$, $\kappa' = \frac{5}{\lambda_2}\frac{\lambda_2+\beta}{\lambda_2^2-25\beta^2} = \kappa\cdot\frac{P}{2m}$, $C_0 = \frac{1}{m}\sum_{k\in[m]}\mathbb{E}\|\nabla L_k(\theta_k^0)-\nabla L_k(\theta_*)\|$ *and*

$$\tilde{\theta}_k^t = \arg\min_\theta L_k(\theta) - \langle\nabla L_k(\theta_k^{t-1}),\theta\rangle + \frac{\lambda_2}{2}\left\|\theta-\theta^{t-1}\right\|_2^2 + \lambda_1\left\|\theta-\theta^{t-1}\right\|_1 \quad \forall k\in[m].$$

Theorem 3.1 provides a convergence rate of FedElasticNet for FedDyn. If $T \to \infty$, the first term of (13) converges to 0 at the speed of $\mathcal{O}(1/T)$. The second and the third terms of (13) are additional penalty terms caused by the ℓ_1-norm regularizer. The second term is a negligible constant in the range of hyperparameters of our interest. Considering the last term, notice that the summand at each t includes the expected average of sign vectors where each element is ±1. If a coordinate of the sign vectors across clients is viewed as an IID realization of Bern($\frac{1}{2}$), it can be thought of as a small value with high probability by the concentration property (see Appendix B.3). In addition, $\gamma^{t-1}-\theta_*$ characterizes how much the average of local models deviates from the globally optimal model, which tends to be small as training proceeds. Therefore, the effect of both additional terms is negligible.

4 Experiments

In this section, we evaluate the proposed FedElasticNet on benchmark datasets for various FL scenarios. In particular, FedElasticNet is integrated with prior methods including FedProx (Li et al., 2020b), SCAFFOLD (Karimireddy et al., 2020), and FedDyn (Acar et al., 2021). The experimental results show that FedElasticNet effectively enhances communication efficiency while maintaining classification accuracy and resolving the client drift problem. We observe that the integration of FedElasticNet and FedDyn (Algorithm 3) achieves the best performance.

Experimental Setup We use the same benchmark datasets as prior works. The evaluated datasets include MNIST (LeCun et al., 1998), a subset of EMNIST (Cohen et al., 2017, EMNIST-L), CIFAR-10, CIFAR-100 (Krizhevsky & Hinton, 2009), and Shakespeare (Shakespeare, 1914). The IID split is generated by randomly assigning datapoint to the local clients. The Dirichlet distribution is used on the label ratios to ensure uneven label distributions among local clients for non-IID splits as in Zhao et al. (2018); Acar et al. (2021). For the uneven label distributions among 100 experimental devices, the experiments are performed by using the Dirichlet parameters of 0.3 and 0.6, and the number of data points is obtained by the lognormal distribution as in Acar et al. (2021). The data imbalance is controlled by varying the variance of the lognormal distribution (Acar et al., 2021).

We use the same neural network models of FedDyn experiments (Acar et al., 2021). For MNIST and EMNIST-L, fully connected neural network architectures with 2 hidden layers are used. The numbers of neurons in the layers are 200 and 100, respectively (Acar et al., 2021). Remark that the model used for MNIST dataset is the same as in Acar et al. (2021); McMahan et al. (2017). For CIFAR-10 and CIFAR-100 datasets, we use a CNN model consisting of 2 convolutional layers with 64 5×5 filters followed by 2 fully connected layers with 394 and 192 neurons and a softmax layer. For the next character prediction task for Shakespeare, we use a stacked LSTM as in Acar et al. (2021).

For MNIST, EMNIST-L, CIFAR10, and CIFAR100 datasets, we evaluate three cases: IID, non-IID with Dirichlet (.6), and non-IID with Dirichlet (.3). Shakespeare datasets are evaluated for IID and non-IID cases as in Acar et al. (2021). We use the batch size of 10 for the MNIST dataset, 50 for CIFAR-10, CIFAR-100, and EMNIST-L datasets, and 20 for the Shakespeare dataset. We optimize the hyperparameters depending on the evaluated datasets: learning rates, λ_2, and λ_1.

	Dataset	Rounds	FedProx	Algorithm 1	SCAFFOLD	Algorithm 2	FedDyn	Algorithm 3
IID	CIFAR-10	200	163.82	**124.56**	327.64	**313.04**	163.82	**34.23**
	CIFAR-100	500	413.37	**249.26**	826.74	**803.33**	413.37	**132.95**
	MNIST	100	20.3	**7.51**	40.58	**36.98**	20.3	**2.55**
	EMNIST-L	200	18.4	**11.23**	36.78	**34.90**	18.4	**2.12**
	Shakespeare	100	1.99	**1.93**	3.32	**3.31**	1.99	**1.28**
Dirichlet (.6)	CIFAR-10	200	163.82	**116.96**	327.64	**310.51**	163.82	**29.96**
	CIFAR-100	500	413.37	**247.87**	826.74	**798.21**	413.37	**127.23**
	MNIST	100	20.3	**6.66**	40.58	**35.20**	20.3	**2.55**
	EMNIST-L	200	18.4	**11.18**	36.78	**34.45**	18.4	**2.05**
Dirichlet (.3)	CIFAR-10	200	163.82	**112.1**	327.64	**308.15**	163.82	**26.99**
	CIFAR-100	500	413.37	**255.97**	826.74	**804.47**	413.37	**124.02**
	MNIST	100	20.3	**6.49**	40.58	**34.95**	20.3	**2.53**
	EMNIST-L	200	18.4	**11.29**	36.78	**34.22**	18.4	**2.07**
Non-IID	Shakespeare	100	13.61	**11.28**	27.21	**27.21**	13.61	**9.41**

Table 2: Number of non-zero elements cumulated over the all round simulated with 10% client participation for IID and non-IID settings in FL scenarios. The non-IID settings of MNIST, EMNIST-L, CIFAR-10, and CIFAR-100 datasets are created with the Dirichlet distribution of labels owned by the client. Algorithm 1 is FedElasticNet for FedProx, Algorithm 2 is FedElasticNet for SCAFFOLD, and Algorithm 3 is FedElasticNet for FedDyn. The unit of the cumulative number of elements is 10^7.

	Dataset	Rounds	FedProx	Algorithm 1	SCAFFOLD	Algorithm 2	FedDyn	Algorithm 3
IID	CIFAR-10	200	586.42	**232.77**	685.17	**236.76**	639.59 (221.64)	**140.71**
	CIFAR-100	500	1712.84	**470.78**	2225.98	**1173.01**	1964.63 (511.14)	**423.53**
	MNIST	100	266.26	**47.29**	286.88	**83.51**	308.27 (27.76)	**24.76**
	EMNIST-L	200	657.64	**166.07**	764.39	**344.94**	704.57 (132.50)	**96.37**
	Shakespeare	100	646.33	**403.63**	520.60	**226.68**	576.17 (348.11)	**225.44**
Dirichlet (.6)	CIFAR-10	200	564.57	**203.61**	663.23	**198.53**	616.69 (197.62)	**121.97**
	CIFAR-100	500	1709.33	**449.59**	2202.61	**1119.91**	1951.06 (478.60)	**398.87**
	MNIST	100	249.63	**45.51**	293.22	**75.57**	304.00 (26.75)	**21.24**
	EMNIST-L	200	646.14	**163.24**	755.75	**347.31**	704.63 (134.31)	**89.92**
Dirichlet (.3)	CIFAR-10	200	550.15	**187.01**	636.90	**115.26**	602.80 (180.29)	**108.69**
	CIFAR-100	500	1696.47	**428.77**	2170.14	**1078.97**	1937.09 (463.67)	**382.44**
	MNIST	100	244.49	**45.24**	291.88	**73.12**	300.76 (26.71)	**19.03**
	EMNIST-L	200	636.21	**162.57**	747.72	**328.21**	700.38 (128.34)	**91.55**
Non-IID	Shakespeare	100	593.21	**440.97**	628.32	**470.22**	609.11 (348.11)	**419.99**

Table 3: Cumulative entropy values of transmitted bits with 10% client participation for IID and non-IID settings in FL scenarios. The non-IID settings of MNIST, EMNIST-L, CIFAR-10, and CIFAR-100 datasets are created with the Dirichlet distribution of labels owned by the client. Algorithm 1 is FedElasticNet for FedProx, Algorithm 2 is FedElasticNet for SCAFFOLD, and Algorithm 3 is FedElasticNet for FedDyn. The left-side numbers of FedDyn are the entropy values when the local models θ_k^t are transmitted and the right-side numbers in parentheses are the entropy values when the local updates $\Delta_k^t = \theta_k^t - \theta^{t-1}$ are transmitted.

Evaluation of Methods We compare the baseline methods (FedProx, SCAFFOLD, and FedDyn) and the proposed FedElasticNet integrations (Algorithms 1, 2, and 3), respectively. We evaluate the communication cost and classification accuracy for non-IID settings of the prior methods and the proposed methods. The robustness of the client drift problem is measured by the classification accuracy of non-IID settings.

We report the communication costs in two ways: (i) the number of nonzero elements in transmitted values as in (Yoon et al., 2021; Jeong et al., 2021) and (ii) the Shannon entropy of transmitted bits. Note that the Shannon entropy is the theoretical limit of data compression (Cover & Thomas, 2006), which can be achieved by practical algorithms; for instance, Han et al. (2016) used Huffman coding for model compression. We calculate the entropy of discretized values with the bin size of 0.01. Note that the transmitted values are not discretized in FL, and only the discretization is considered to calculate the entropy. The lossy compression schemes (e.g., scalar quantization, vector quantization, etc.) have not been considered since they include several implementational issues which are beyond our research scope.

Table 2 reports the number of non-zero elements of the baseline methods with/without FedElasticNet. Basically, the communication costs per round of FedProx and FedDyn are the same; SCAFFOLD suffers from the doubled communication cost because of the control variates. The proposed FedElasticNet integrations (Algorithms 1, 2, and 3) can effectively sparsify the transmitted local updates, which enhances communication efficiency.

	Dataset	Rounds	FedProx	Algorithm 1	SCAFFOLD	Algorithm 2	FedDyn	Algorithm 3
IID	CIFAR-10	200	595.16	**151.28**	873.24	**252.33**	680.70 (259.31)	**57.70**
	CIFAR-100	500	1721.53	**466.21**	2774.60	**1068.47**	2038.07 (689.24)	**447.18**
	MNIST	100	325.86	**39.55**	389.52	**71.57**	324.88 (20.47)	**12.33**
	EMNIST-L	200	728.34	**123.74**	1018.11	**263.95**	797.39 (55.46)	**40.71**
	Shakespeare	100	640.69	**279.51**	529.05	**476.81**	343.32 (298.58)	**277.21**
Dirichlet (.6)	CIFAR-10	200	577.74	**127.14**	839.41	**236.48**	656.48 (223.46)	**47.52**
	CIFAR-100	500	1697.18	**453.87**	2682.15	**1038.21**	1974.65 (651.78)	**431.54**
	MNIST	100	298.99	**30.94**	530.72	**106.08**	314.64 (20.29)	**11.67**
	EMNIST-L	200	721.49	**121.76**	1020.32	**251.65**	779.44 (286.11)	**40.71**
Dirichlet (.3)	CIFAR-10	200	563.15	**105.89**	806.73	**214.31**	635.78 (215.83)	**39.58**
	CIFAR-100	500	1685.30	**444.32**	2743.43	**1060.83**	1934.49 (627.56)	**422.46**
	MNIST	100	295.80	**42.94**	466.65	**85.06**	314.96 (19.98)	**12.35**
	EMNIST-L	200	716.12	**116.88**	1014.08	**249.68**	771.90 (283.40)	**40.70**
Non-IID	Shakespeare	100	595.69	**409.60**	**684.79**	897.67	560.87 (316.64)	**318.92**

Table 4: Cumulative entropy values of transmitted bits with 100% client participation for IID and non-IID settings in FL scenarios. The non-IID settings of MNIST, EMNIST-L, CIFAR-10, and CIFAR-100 datasets are created with the Dirichlet distribution of labels owned by the client. Algorithm 1 is FedElasticNet for FedProx, Algorithm 2 is FedElasticNet for SCAFFOLD, and Algorithm 3 is FedElasticNet for FedDyn. The left-side numbers of FedDyn are the entropy values when the local models θ_k^t are transmitted and the right-side numbers in parentheses are the entropy values when the local updates $\Delta_k^t = \theta_k^t - \theta^{t-1}$ are transmitted.

In particular, the minimal communication cost is achieved when FedElasticNet is integrated with FedDyn (Algorithm 3). It is because the classification accuracy is not degraded even if the transmitted values are more aggressively sparsified in Algorithm 3. Fig. 2 shows the transmitted local updates Δ_k^t of Algorithm 3 are sparser than FedDyn and Algorithm 2. Hence, Algorithm 3 (FedElasticNet for FedDyn) achieves the best communication efficiency.

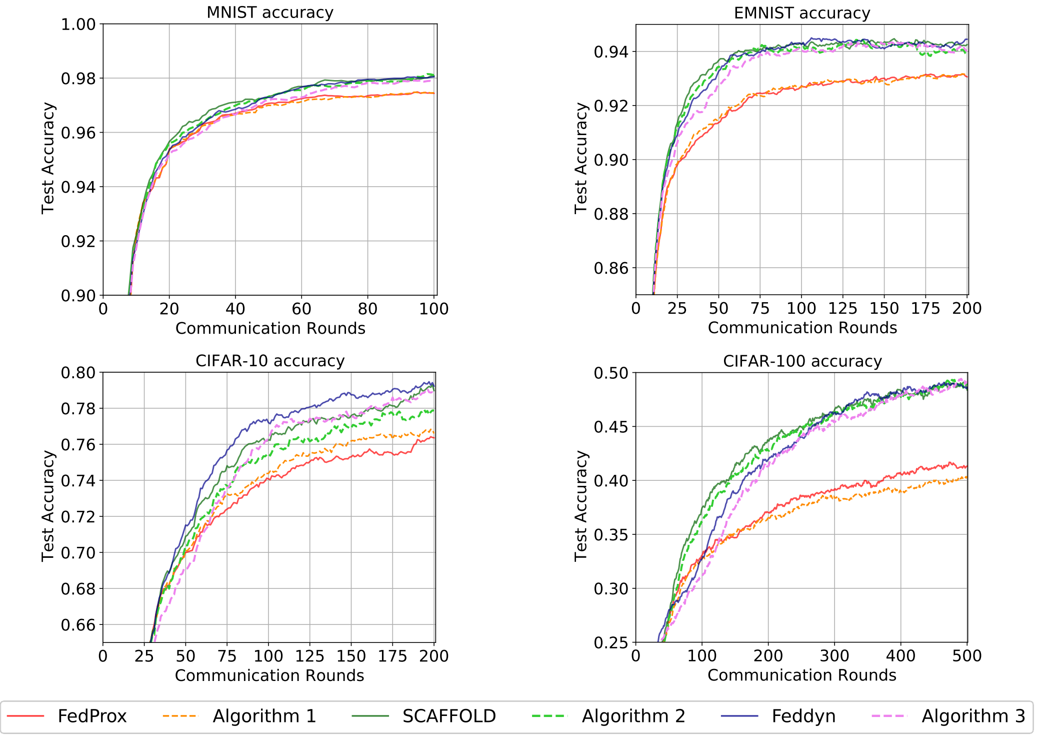

Figure 1: Classification accuracy performance evaluated in MNIST, EMNIST-L, CIFAR-10, CIFAR-100 dataset settings (10% participation rate and Dirichlet (.3)).

Tables 3 and 4 report the Shannon entropy of transmitted bits for the baseline methods with/without FedElasticNet. The communication costs of baseline methods are effectively improved by the

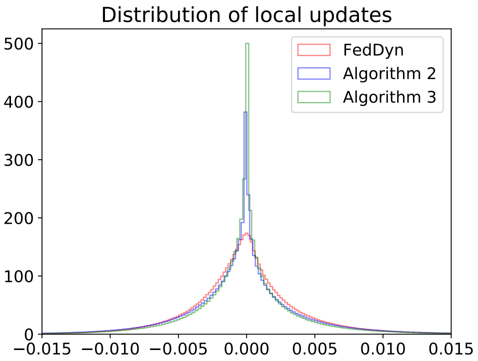

Figure 2: Comparison of distributions of transmitted local updates $\Delta_k^t = \theta_k^t - \theta^{t-1}$ (10% participation rate and Dirichlet (.3)) for CIFAR-10.

FedElasticNet approach. Algorithms 1, 2, and 3 reduce the entropy compared to the their baseline methods. We note that FedElasticNet integrated with FedDyn (Algorithm 3) achieves the minimum entropy, i.e., the minimum communication cost.

For FedDyn, we evaluate the Shannon entropy values for two cases: (i) transmit the updated local models θ_k^t as in Acar et al. (2021) and (ii) transmit the local updates $\Delta_k^t = \theta_k^t - \theta^{t-1}$ as in Algorithm 3. We observe that transmitting the local updates Δ_k^t instead of the local models θ_k^t can reduce the Shannon entropy significantly. Hence, it is beneficial to transmit the local updates Δ_k^t even for FedDyn if it adopts an additional compression scheme. The numbers of nonzero elements for two cases (i.e., θ_k^t and Δ_k^t) are the same for FedDyn.

Fig. 1 shows that the FedElasticNet maintains the classification accuracy or incurs marginal degradation. We observe a classification gap between FedProx and Algorithm 1 for CIFAR-10 and CIFAR-100. However, the classification accuracies of FedDyn and Algorithm 3 are almost identical in the converged regime.

In particular, Algorithm 3 significantly reduces the Shannon entropy, which can be explained by Fig 2. Fig 2 compares the distributions of the transmitted local updates Δ_k^t for FedDyn, Algorithm 2, and Algorithm 3. Because of the ℓ_1-norm penalty on the local updates, Algorithm 3 makes sparser local updates than FedDyn. The local updates of FedDyn can be modeled by the Gaussian distribution, and the local updates of FedElasticNet can be modeled by the non-Gaussian distribution (similar to the Laplacian distribution). It is well-known that the Gaussian distribution maximizes the entropy for a given variance in information theory Cover & Thomas (2006). Hence, FedElasticNet can reduce the entropy by transforming the Gaussian distribution into the non-Gaussian one.

5 Conclusion

We proposed FedElasticNet, a general framework to improve communication efficiency and resolve the client drift problem simultaneously. We introduce two types of penalty terms on the local model updates by repurposing the classical elastic net. The ℓ_1-norm regularizer sparsifies the local model updates, which reduces the communication cost. The ℓ_2-norm regularizer limits the impact of variable local updates to resolve the client drift problem. Importantly, our framework can be integrated with prior FL techniques so as to simultaneously resolve the communication cost problem and the client drift problem. By integrating FedElasticNet with FedDyn, we can achieve the best communication efficiency while maintaining classification accuracy for heterogeneous datasets.

References

Durmus Alp Emre Acar, Yue Zhao, Ramon Matas, Matthew Mattina, Paul Whatmough, and Venkatesh Saligrama. Federated learning based on dynamic regularization. In *International Conference on Learning Representations (ICLR)*, May 2021.

Keith Bonawitz, Hubert Eichner, Wolfgang Grieskamp, Dzmitry Huba, Alex Ingerman, Vladimir Ivanov, Chloé Kiddon, Jakub Konečný, Stefano Mazzocchi, Brendan McMahan, Timon Van Overveldt, David Petrou, Daniel Ramage, and Jason Roselander. Towards federated learning at scale: System design. In A Talwalkar, V Smith, and M Zaharia (eds.), *Proceedings of Machine Learning and Systems*, volume 1, pp. 374–388, 2019.

Gregory Cohen, Saeed Afshar, Jonathan Tapson, and Andre Van Schaik. Emnist: Extending mnist to handwritten letters. In *International Joint Conference on Neural Networks (IJCNN)*, pp. 2921–2926, 2017.

Thomas M. Cover and Joy A. Thomas. *Elements of information theory*. Wiley-Interscience, New York, 2006.

Rick Durrett. *Probability: Theory and Examples*. Cambridge University Press, Cambridge, UK, fifth edition, 2019. doi: 10.1017/9781108591034.

Song Han, Huizi Mao, and William J. Dally. Deep compression: Compressing deep neural networks with pruning, trained quantization and huffman coding. In *International Conference on Learning Representations (ICLR)*, volume abs/1510.0, October 2016.

Jianhua Hu, Jian Huang, and Feng Qiu. A group adaptive elastic-net approach for variable selection in high-dimensional linear regression. *Science China Mathematics*, 61(1):173–188, 2018.

Wonyong Jeong, Jaehong Yoon, Eunho Yang, and Sung Ju Hwang. Federated semi-supervised learning with inter-client consistency & disjoint learning. In *International Conference on Learning Representations (ICLR)*, 2021.

Peter Kairouz, H. Brendan McMahan, Brendan Avent, Aurélien Bellet, Mehdi Bennis, Arjun Nitin Bhagoji, Kallista Bonawitz, Zachary Charles, Graham Cormode, Rachel Cummings, et al. Advances and open problems in federated learning. *Foundations and Trends® in Machine Learning*, 14(1–2):1–210, 2021.

Sai Praneeth Karimireddy, Satyen Kale, Mehryar Mohri, Sashank Reddi, Sebastian Stich, and Ananda Theertha Suresh. Scaffold: Stochastic controlled averaging for federated learning. In *International Conference on Machine Learning (ICML)*, pp. 5132–5143, 2020.

Jakub Konečǹy, H. Brendan McMahan, Daniel Ramage, and Peter Richtárik. Federated optimization: Distributed machine learning for on-device intelligence. *arXiv preprint arXiv:1610.02527*, 2016a.

Jakub Konečǹy, H. Brendan McMahan, Felix X. Yu, Peter Richtárik, Ananda Theertha Suresh, and Dave Bacon. Federated learning: Strategies for improving communication efficiency. *arXiv preprint arXiv:1610.05492*, 2016b.

Alex Krizhevsky and Geoffrey Hinton. Learning multiple layers of features from tiny images. Technical report, University of Toronto, 2009.

Yann LeCun, Léon Bottou, Yoshua Bengio, and Patrick Haffner. Gradient-based learning applied to document recognition. *Proceedings of the IEEE*, 86(11):2278–2324, 1998.

Tian Li, Anit Kumar Sahu, Ameet Talwalkar, and Virginia Smith. Federated learning: Challenges, methods, and future directions. *IEEE Signal Processing Magazine*, 37(3):50–60, 2020a.

Tian Li, Anit Kumar Sahu, Manzil Zaheer, Maziar Sanjabi, Ameet Talwalkar, and Virginia Smith. Federated optimization in heterogeneous networks. In *Proceedings of Machine Learning and Systems*, volume 2, pp. 429–450, 2020b.

Grigory Malinovskiy, Dmitry Kovalev, Elnur Gasanov, Laurent Condat, and Peter Richtarik. From local sgd to local fixed-point methods for federated learning. In *International Conference on Machine Learnin (ICML)*, pp. 6692–6701, 2020.

H. Brendan McMahan, Eider Moore, Daniel Ramage, Seth Hampson, and Blaise Aguera y Arcas. Communication-efficient learning of deep networks from decentralized data. In *International Conference on Artificial Intelligence and Statistics (AISTATS)*, pp. 1273–1282. PMLR, 2017.

Y. Nesterov. *Lectures on convex optimization*, volume 137. springer, 2018. URL https://link.springer.com/content/pdf/10.1007/978-3-319-91578-4.pdf.

Amirhossein Reisizadeh, Aryan Mokhtari, Hamed Hassani, Ali Jadbabaie, and Ramtin Pedarsani. FedPAQ: A communication-efficient federated learning method with periodic averaging and quantization. In *International Conference on Artificial Intelligence and Statistics (AISTATS)*, volume 108, pp. 2021–2031, August 2020.

William Shakespeare. *The complete works of William Shakespeare*. Humphrey Milford, Oxford University Press, 1914. URL http://www.gutenberg.org/files/100/old/1994-01-100.zip.

Robert Tibshirani. Regression shrinkage and selection via the lasso. *Journal of the Royal Statistical Society: Series B (Methodological)*, 58(1):267–288, 1996.

Jinjin Xu, Wenli Du, Yaochu Jin, Wangli He, and Ran Cheng. Ternary compression for communication-efficient federated learning. *IEEE Transactions on Neural Networks and Learning Systems*, 2020.

Jaehong Yoon, Wonyong Jeong, Giwoong Lee, Eunho Yang, and Sung Ju Hwang. Federated continual learning with weighted inter-client transfer. In Marina Meila and Tong Zhang (eds.), *International Conference on Machine Learning (ICML)*, volume 139 of *Proceedings of Machine Learning Research*, pp. 12073–12086, 2021.

Yue Zhao, Meng Li, Liangzhen Lai, Naveen Suda, Damon Civin, and Vikas Chandra. Federated learning with non-iid data. *arXiv preprint arXiv:1806.00582*, 2018.

Hui Zou and Trevor Hastie. Regularization and variable selection via the elastic net. *Journal of the Royal Statistical Society: Series B (Statistical Methodology)*, 67(2):301–320, 2005.

A Appendix

A.1 Experiment Details

We provide the details of our experiments. We select the datasets for our experiments, including those used in prior work on federated learning (McMahan et al., 2017; Li et al., 2020b; Acar et al., 2021). To fairly compare the non-IID environments, the datasets and the experimental environments are the same as those of Acar et al. (2021).

Hyperparameters. We describe the hyperparameters used in our experiments in Section 4. We perform a grid search to find the best λ_1 and ϵ used in the proposed algorithms. Each hyperparameter was selected to double the value as the performance improved. We use the same λ_2 as in Acar et al. (2021). SCAFFOLD has the same local epoch and batch size as other algorithms, and SCAFFOLD is not included in Table 4 because other hyperparameters are not required. Table 5 shows the hyperparameters used in our experiments.

Dataset	Algorithm	λ_1	λ_2	ϵ
CIFAR-10	FedProx	-	10^{-4}	-
	Algorithm 1	10^{-6}	10^{-4}	10^{-3}
	Algorithm 2	10^{-4}	0	10^{-4}
	FedDyn	-	10^{-2}	-
	Algorithm 3	10^{-4}	10^{-2}	5×10^{-3}
CIFAR-100	FedProx	-	10^{-4}	-
	Algorithm 1	10^{-6}	10^{-4}	10^{-3}
	Algorithm 2	10^{-4}	0	10^{-4}
	FedDyn	-	10^{-2}	-
	Algorithm 3	10^{-4}	10^{-2}	10^{-3}
MNIST	FedProx	-	10^{-4}	-
	Algorithm 1	10^{-6}	10^{-6}	10^{-3}
	Algorithm 2	10^{-4}	0	10^{-4}
	FedDyn	-	5×10^{-2}	-
	Algorithm 3	10^{-4}	5×10^{-2}	5×10^{-3}
EMNIST-L	FedProx	-	10^{-4}	-
	Algorithm 1	10^{-6}	10^{-6}	10^{-3}
	Algorithm 2	10^{-4}	0	10^{-4}
	FedDyn	-	4×10^{-2}	-
	Algorithm 3	10^{-4}	4×10^{-2}	2×10^{-3}
Shakespeare	FedProx	-	10^{-4}	-
	Algorithm 1	10^{-6}	10^{-6}	9×10^{-3}
	Algorithm 2	10^{-6}	0	9×10^{-4}
	FedDyn	-	10^{-2}	-
	Algorithm 3	10^{-6}	10^{-2}	10^{-2}

Table 5: Hyperparameters.

A.2 Regularizer Coefficients

We selected λ_1 over $\{10^{-2}, 10^{-4}, 10^{-6}, 10^{-8}\}$ to observe the impact of λ_1 on the classification accuracy. We prefer a larger λ_1 to enhance communication efficiency unless the ℓ_1-norm regularizer does not degrade the classification accuracy. Figures 3, 4, and 5 show the classification accuracy depending on λ_1 in the CIFAR-10 dataset with 10% participation rate and Dirichlet (.3). The unit of the cumulative number of elements is 10^7.

In Algorithm 1, we selected $\lambda_1 = 10^{-6}$ to avoid a degradation of classification accuracy (see Fig. 3) and maximize the sparsity of local updates. In this way, we selected the coefficient values λ_1 (See Fig.4 for Algorithm 2 and 5 and Algorithm 3).

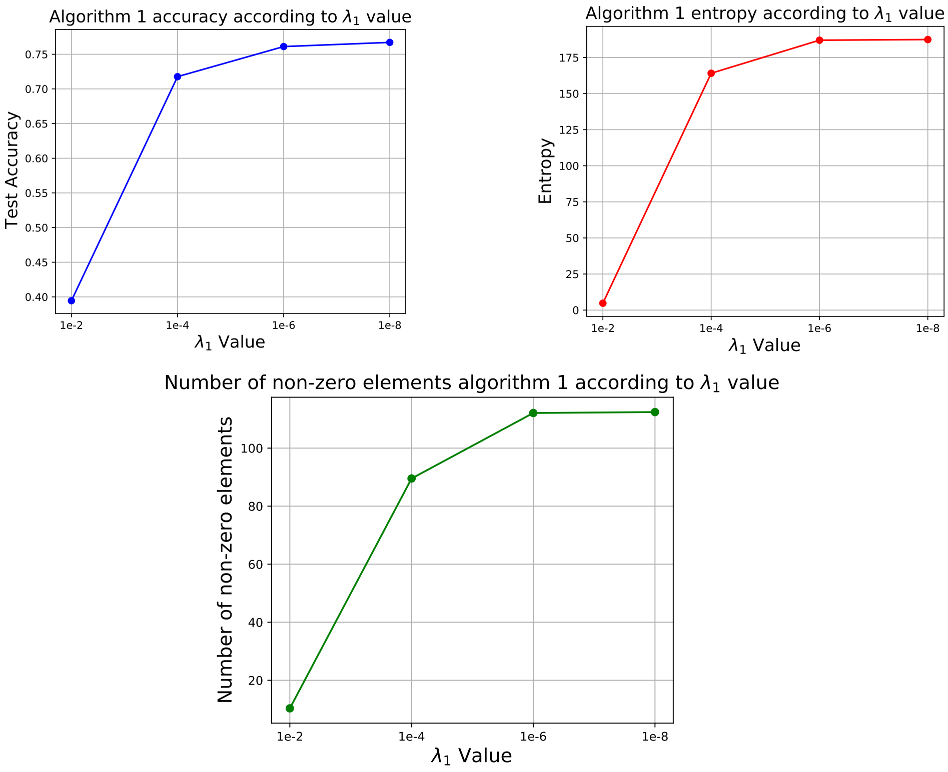

Figure 3: Classification accuracy and sparsity of local updates depending on λ_1 (Algorithm 1).

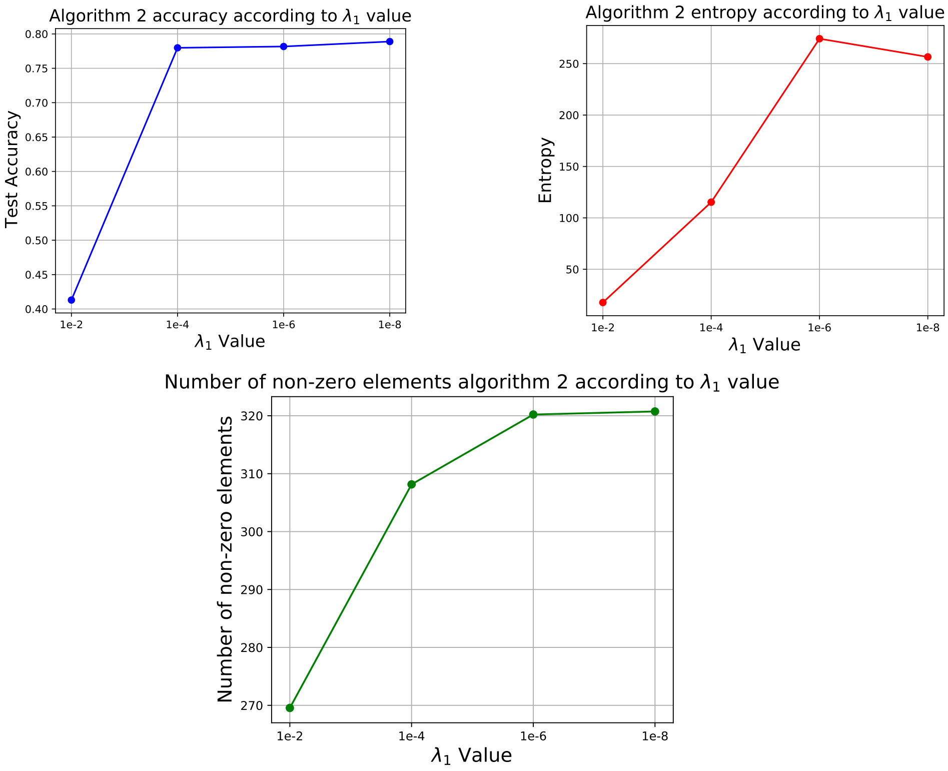

Figure 4: Classification accuracy and sparsity of local updates depending on λ_1 (Algorithm 2).

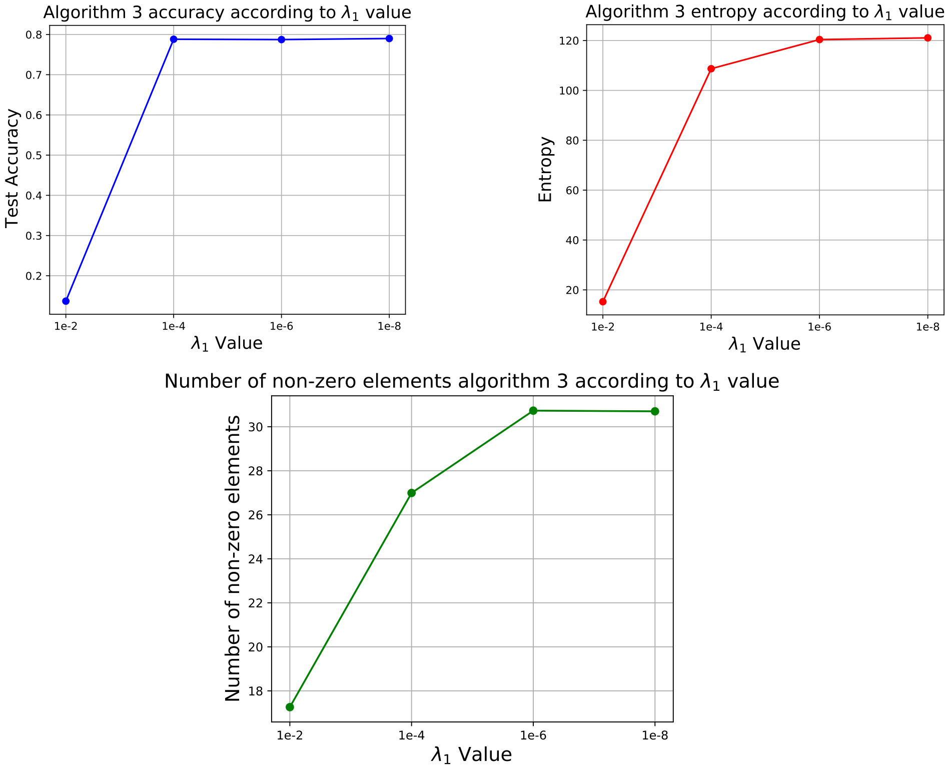

Figure 5: Classification accuracy and sparsity of local updates depending on λ_1 (Algorithm 3).

A.3 Empirical Results of Classification Accuracy

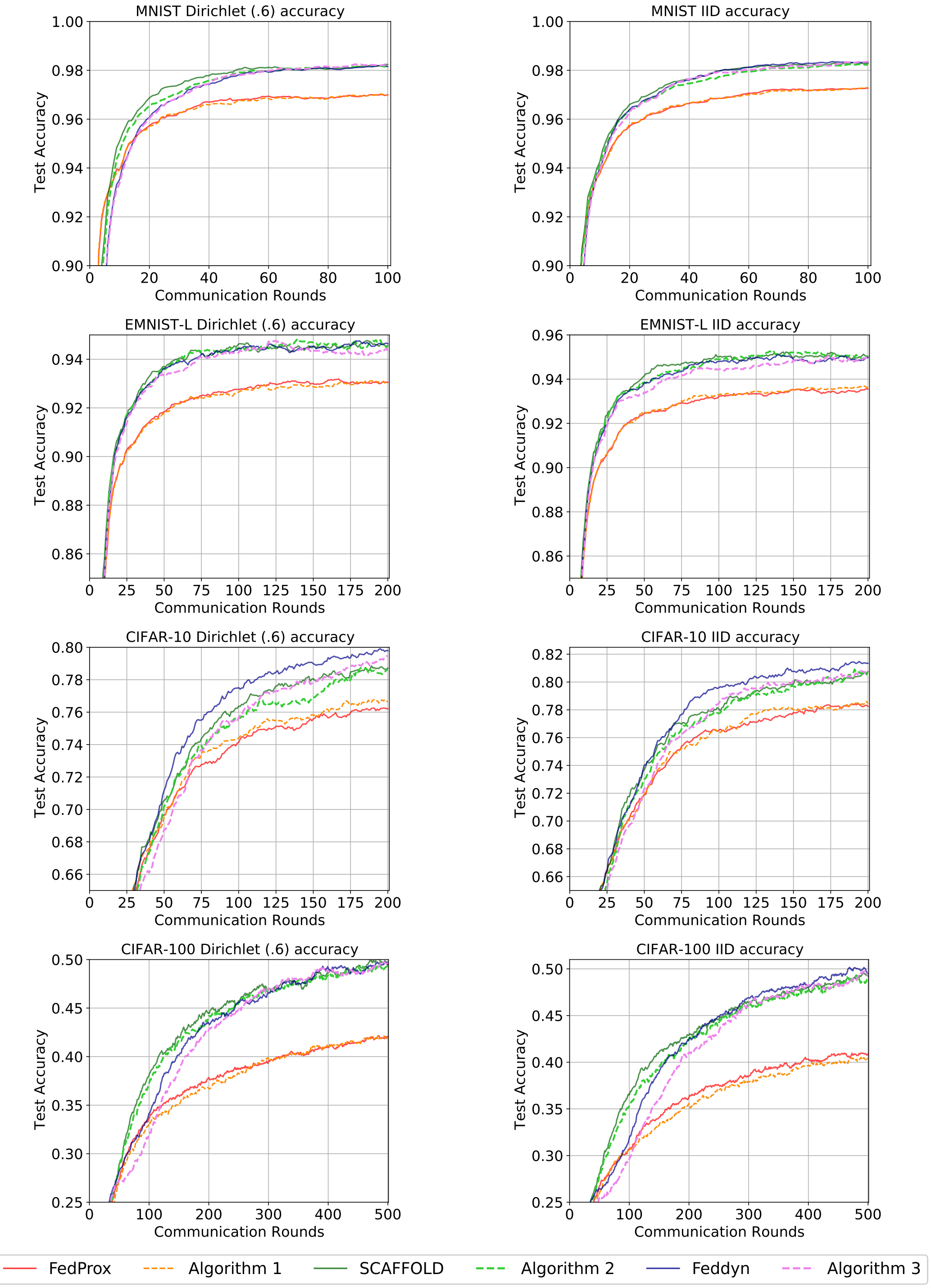

Figure 6: Classification accuracy performance evaluated in MNIST, EMNIST-L, CIFAR-10, and CIFAR-100 datasets (10% participation rate).

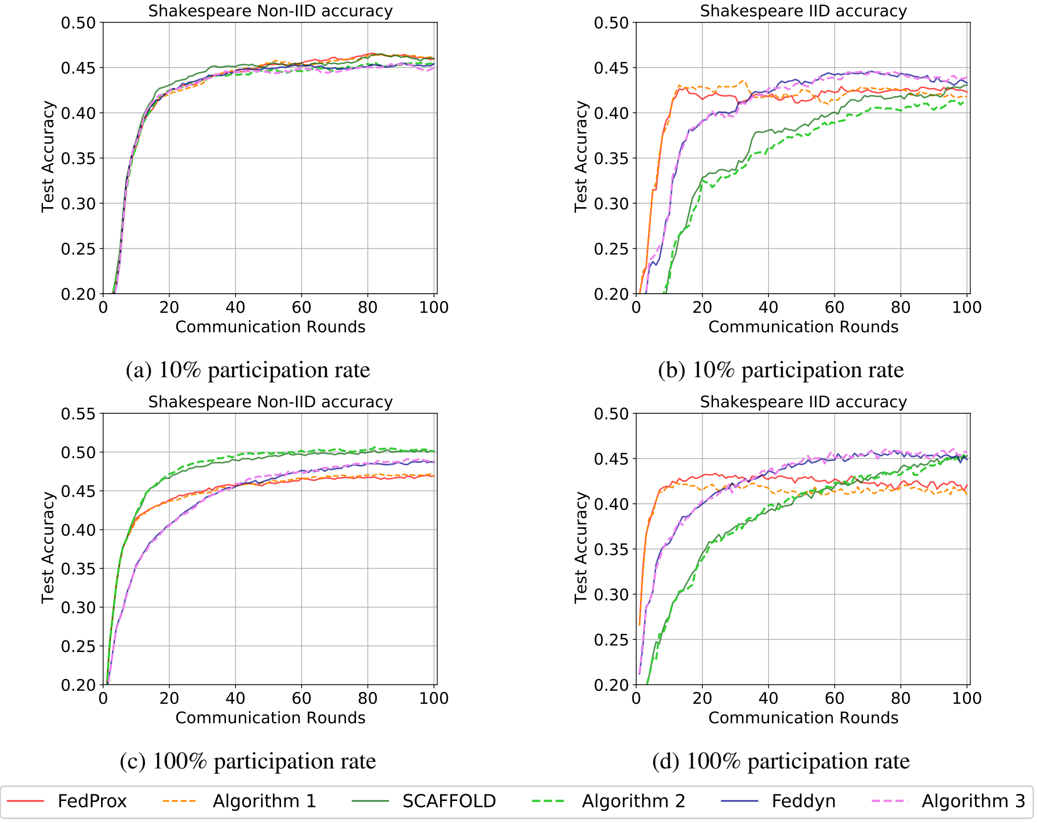

(a) 10% participation rate

(b) 10% participation rate

(c) 100% participation rate

(d) 100% participation rate

Figure 7: Classification accuracy performance evaluated in IID Shakespeare and Non-IID Shakespeare datasets.

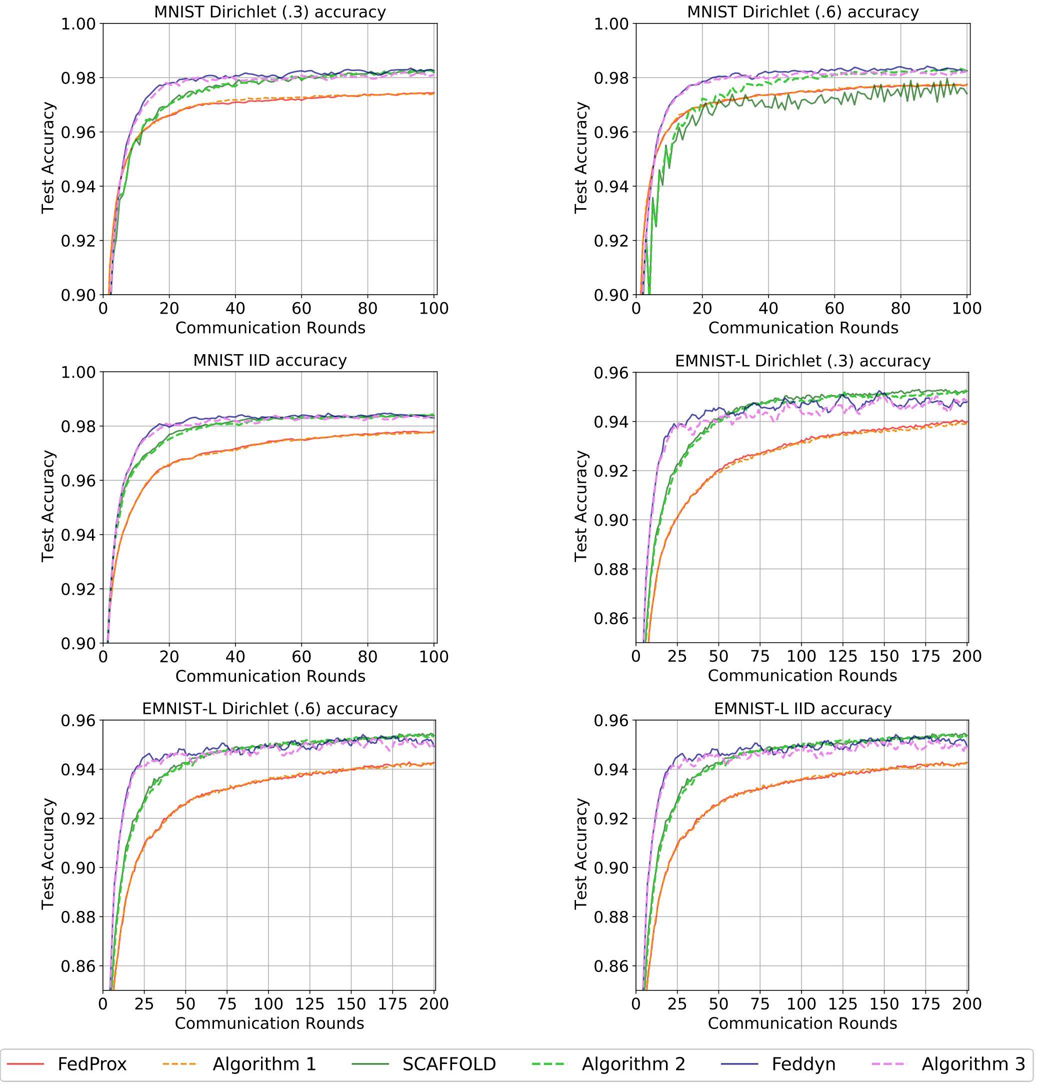

Figure 8: Classification accuracy performance evaluated in MNIST, EMNIST-L datasets (100% participation rate).

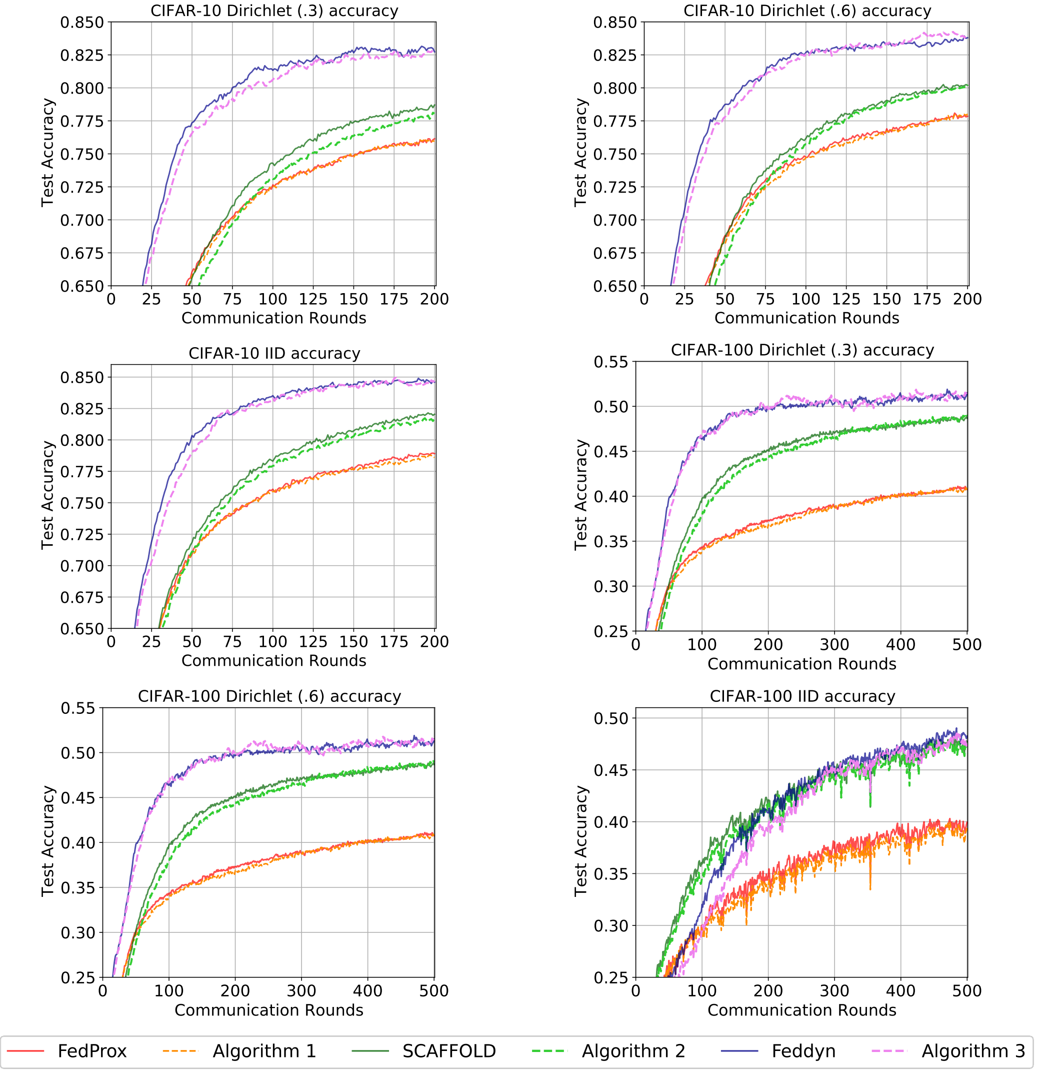

Figure 9: Classification accuracy performance evaluated in CIFAR-10 and CIFAR-100 datasets (100% participation rate).

B Proof

We utilize some techniques in FedDyn (Acar et al., 2021).

B.1 Definition

We introduce a formal definition and properties that we will use.

Definition B.0.1. *A function L_k is β-smooth if it satisfies*

$$\|\nabla L_k(x) - \nabla L_k(y)\| \leq \beta\|x - y\| \quad \forall x, y. \tag{14}$$

If function L_k is convex and β-smooth, it satisfies

$$-\langle \nabla L_k(x), z - y\rangle \leq -L_k(z) + L_k(y) + \frac{\beta}{2}\|z - x\|^2 \;\; \forall x, y, z. \tag{15}$$

As a consequence of the convexity and smoothness, the following property holds (Nesterov, 2018, Theorem 2.1.5):

$$\frac{1}{2\beta m}\sum_{k\in[m]}\|\nabla L_k(x) - \nabla L_k(x_*)\|^2 \leq \mathcal{R}(x) - \mathcal{R}(x_*) \;\; \forall x \tag{16}$$

where $\mathcal{R}(x) = \frac{1}{m}\sum_{k=1}^m L_k(x)$ and $\nabla\mathcal{R}(x_*) = 0$.

We will also use the relaxed triangle inequality (Karimireddy et al., 2020, Lemma 3):

$$\left\|\sum_{j=1}^n v_j\right\|^2 \leq n\sum_{j=1}^n\|v_j\|^2. \tag{17}$$

B.2 Proof of Theorem 3.1

The theorem that we will prove is as follows.

Theorem B.1 (Full statement of Theorem 3.1)**.** *Assume that the clients are uniformly randomly selected at each round and the individual loss functions $\{L_k\}_{k=1}^m$ are convex and β-smooth. Also assume that $\lambda_2 > 27\beta$. Then Algorithm 3 satisfies the following inequality: Letting $\mathcal{R}(\theta) = \frac{1}{m}\sum_{k\in[m]} L_k(\theta)$ and $\theta_* = \arg\min_\theta \mathcal{R}(\theta)$,*

$$\begin{aligned}\mathbb{E}\left[\mathcal{R}\left(\frac{1}{T}\sum_{t=0}^{T-1}\gamma^t\right) - \mathcal{R}(\theta_*)\right] \leq \frac{1}{T}\frac{1}{\kappa_0}(\mathbb{E}\|\gamma^0 - \theta_*\|^2 + \kappa C_0) + \frac{\kappa'}{\kappa_0}\cdot\lambda_1^2 d \\ - \frac{1}{T}\frac{2\lambda_1}{\lambda_2}\sum_{t=1}^T\left\langle(\gamma^{t-1} - \theta_*), \frac{1}{m}\sum_{k\in[m]}\mathbb{E}[\text{sign}(\tilde{\theta}_k^t - \theta^{t-1})]\right\rangle,\end{aligned} \tag{18}$$

where

$$\begin{aligned}\gamma^t &= \frac{1}{P}\sum_{k\in\mathcal{P}_t}\theta_k^t = \theta^t + \frac{1}{\lambda_2}h^t \quad \textit{with } P = |\mathcal{P}_t|,\\ \kappa &= \frac{10m}{P}\frac{1}{\lambda_2}\frac{\lambda_2 + \beta}{\lambda_2^2 - 25\beta^2},\\ \kappa_0 &= \frac{2}{\lambda_2}\frac{\lambda_2^2 - 25\lambda_2\beta - 50\beta^2}{\lambda_2^2 - 25\beta^2},\\ \kappa' &= \frac{5}{\lambda_2}\frac{\lambda_2 + \beta}{\lambda_2^2 - 25\beta^2} = \kappa\cdot\frac{P}{2m},\\ C_0 &= \frac{1}{m}\sum_{k\in[m]}\mathbb{E}\|\nabla L_k(\theta_k^0) - \nabla L_k(\theta_*)\|,\\ d &= \mathit{dim}(\theta).\end{aligned}$$

To prove the theorem, define variables that will be used throughout the proof.

$$\tilde{\theta}_k^t = \arg\min_\theta L_k(\theta) - \left\langle \nabla L_k(\theta_k^{t-1}), \theta \right\rangle + \frac{\lambda_2}{2} \left\| \theta - \theta^{t-1} \right\|_2^2 + \lambda_1 \left\| \theta - \theta^{t-1} \right\|_1 \quad \forall k \in [m] \tag{19}$$

$$C_t = \frac{1}{m} \sum_{k \in [m]} \mathbb{E} \| \nabla L_k(\theta_k^t) - \nabla L_k(\theta_*) \|^2, \tag{20}$$

$$\epsilon_t = \frac{1}{m} \sum_{k \in [m]} \mathbb{E} \| \tilde{\theta}_k^t - \gamma^{t-1} \|^2. \tag{21}$$

Note that $\tilde{\theta}_k^t$ optimizes the kth loss function by assuming that the kth client ($k \in [m]$) is selected at round t. It is obvious that $\tilde{\theta}_k^t = \theta_k^t$ if $k \in \mathcal{P}_t$. C_t refers to the average of the expected differences between gradients of each individual model and the globally optimal model. Lastly, ϵ_t refers to the deviation of each client model from the average of local models. Remark that C_t and ϵ_t approach zero if all clients' models converge to the globally optimal model, i.e., $\theta_k^t \to \theta_*$.

The following lemma expresses h^t, how much the averaged active devices' model deviates from the global model.

Lemma B.2. *Algorithm 3 satisfies*

$$h^t = \frac{1}{m} \sum_{k \in [m]} \nabla L_k(\theta_k^t) \tag{22}$$

Proof. Starting from the update of h^t in Algorithm 3,

$$\begin{aligned}
h^t &= h^{t-1} - \frac{\lambda_2}{m} \sum_{k \in [m]} (\theta_k^t - \theta^{t-1}) - \frac{\lambda_1}{m} \sum_{k \in [m]} \mathrm{sign}(\theta_k^t - \theta^{t-1}) \\
&= h^{t-1} - \frac{1}{m} \sum_{k \in [m]} (\nabla L_k(\theta_k^{t-1}) - \nabla L_k(\theta_k^t) - \lambda_1 \mathrm{sign}(\theta_k^t - \theta^{t-1})) - \frac{\lambda_1}{m} \sum_{k \in [m]} \mathrm{sign}(\theta_k^t - \theta^{t-1}) \\
&= h^{t-1} - \frac{1}{m} \sum_{k \in [m]} (\nabla L_k(\theta_k^{t-1}) - \nabla L_k(\theta_k^t)),
\end{aligned}$$

where the second equality follows from (11). By summing h^t recursively, we have

$$h^t = h^0 + \frac{1}{m} \sum_{k \in [m]} \nabla L_k(\theta_k^t) - \frac{1}{m} \sum_{k \in [m]} \nabla L_k(\theta_k^0) = \frac{1}{m} \sum_{k \in [m]} \nabla L_k(\theta_k^t).$$

□

The next lemma provides how much the average of local models changes by using only t round parameters.

Lemma B.3. *Algorithm 3 satisfies*

$$\mathbb{E}[\gamma^t - \gamma^{t-1}] = \frac{1}{\lambda_2 m} \sum_{k \in [m]} \mathbb{E}[-\nabla L_k(\tilde{\theta}_k^t)] - \frac{\lambda_1}{\lambda_2 m} \sum_{k \in [m]} \mathbb{E}[\mathrm{sign}(\tilde{\theta}_k^t - \theta^{t-1})].$$

Proof. Starting from the definition of γ^t,

$$
\begin{aligned}
\mathbb{E}\left[\gamma^t - \gamma^{t-1}\right] &= \mathbb{E}\left[\left(\frac{1}{P}\sum_{k\in\mathcal{P}_t}\theta_k^t\right) - \theta^{t-1} - \frac{1}{\lambda_2}h^{t-1}\right] \\
&= \mathbb{E}\left[\frac{1}{P}\sum_{k\in\mathcal{P}_t}(\theta_k^t - \theta^{t-1}) - \frac{1}{\lambda_2}h^{t-1}\right] \\
&= \mathbb{E}\left[\frac{1}{\lambda_2 P}\sum_{k\in\mathcal{P}_t}(\nabla L_k(\theta_k^{t-1}) - \nabla L_k(\theta_k^t) - \lambda_1 \mathrm{sign}(\theta_k^t - \theta^{t-1})) - \frac{1}{\lambda_2}h^{t-1}\right] \quad (23) \\
&= \mathbb{E}\left[\frac{1}{\lambda_2 P}\sum_{k\in\mathcal{P}_t}(\nabla L_k(\theta_k^{t-1}) - \nabla L_k(\tilde{\theta_k^t}) - \lambda_1 \mathrm{sign}(\tilde{\theta_k^t} - \theta^{t-1})) - \frac{1}{\lambda_2}h^{t-1}\right] \quad (24) \\
&= \mathbb{E}\left[\frac{1}{\lambda_2 m}\sum_{k\in[m]}(\nabla L_k(\theta_k^{t-1}) - \nabla L_k(\tilde{\theta_k^t}) - \lambda_1 \mathrm{sign}(\tilde{\theta_k^t} - \theta^{t-1})) - \frac{1}{\lambda_2}h^{t-1}\right] \\
&\qquad (25) \\
&= \frac{1}{\lambda_2 m}\sum_{k\in[m]}\mathbb{E}[-\nabla L_k(\tilde{\theta_k^t})] - \frac{\lambda_1}{\lambda_2 m}\sum_{k\in[m]}\mathbb{E}[\mathrm{sign}(\tilde{\theta_k^t} - \theta^{t-1})], \quad (26)
\end{aligned}
$$

where (23) follows from (11), (24) follows since $\tilde{\theta}_k^t = \theta_k^t$ if $k \in \mathcal{P}_t$, and (25) follows since clients are randomly chosen. The last equality is due to Lemma B.2. □

Next, note that Algorithm 3 is the same as that of FedDyn except for the ℓ_1-norm penalty. As this new penalty does not affect derivations of C_t, ϵ_t, and $\mathbb{E}\|\gamma^t - \gamma^{t-1}\|^2$ in FedDyn (Acar et al., 2021), we can obtain the following bounds on them. Proofs are omitted for brevity.

$$
\begin{aligned}
&\mathbb{E}\|h^t\|^2 \le C_t \quad (27) \\
&C_t \le \left(1 - \frac{P}{m}\right)C_{t-1} + \frac{2\beta^2 P}{m}\epsilon_t + \frac{4\beta P}{m}\mathbb{E}[\mathcal{R}(\gamma^{t-1}) - \mathcal{R}(\theta_*)] \quad (28) \\
&\mathbb{E}\|\gamma^t - \gamma^{t-1}\|^2 \le \frac{1}{m}\sum_{k\in[m]}\mathbb{E}[\|\tilde{\theta_k^t} - \gamma^{t-1}\|^2] = \epsilon_t \quad (29)
\end{aligned}
$$

Lemma B.4. *Given model parameters at the round $(t-1)$, Algorithm 3 satisfies*

$$
\begin{aligned}
\mathbb{E}\|\gamma^t - \theta_*\|^2 \le &\mathbb{E}\|\gamma^{t-1} - \theta_*\|^2 - \frac{2}{\lambda_2}\mathbb{E}[\mathcal{R}(\gamma^{t-1}) - \mathcal{R}(\theta_*)] + \frac{\beta}{\lambda_2}\epsilon_t + \mathbb{E}\|\gamma^t - \gamma^{t-1}\|^2 \quad (30) \\
&- \frac{2\lambda_1}{\lambda_2 m}(\gamma^{t-1} - \theta_*)\sum_{k\in[m]}\mathbb{E}[sign(\tilde{\theta_k^t} - \theta^{t-1})], \quad (31)
\end{aligned}
$$

where the expectations are taken assuming parameters at the round $(t-1)$ are given.

Proof.

$$
\begin{aligned}
\mathbb{E}\|\gamma^t - \theta_*\|^2 &= \mathbb{E}\|\gamma^{t-1} - \theta_* + \gamma^t - \gamma^{t-1}\|^2 \\
&= \mathbb{E}\|\gamma^{t-1} - \theta_*\|^2 + 2\mathbb{E}[\langle \gamma^{t-1} - \theta_*, \gamma^t - \gamma^{t-1}\rangle] + \mathbb{E}\|\gamma^t - \gamma^{t-1}\|^2 \\
&= \mathbb{E}\|\gamma^{t-1} - \theta_*\|^2 + \mathbb{E}\|\gamma^t - \gamma^{t-1}\|^2 \\
&\quad + \frac{2}{\lambda_2 m}\sum_{k\in[m]}\mathbb{E}\left[\left\langle \gamma^{t-1} - \theta_*, -\nabla L_k(\tilde{\theta}_k^t) - \lambda_1(\text{sign}(\tilde{\theta}_k^t - \theta^{t-1}))\right\rangle\right] \qquad (32) \\
&\leq \mathbb{E}\|\gamma^{t-1} - \theta_*\|^2 + \mathbb{E}\|\gamma^t - \gamma^{t-1}\|^2 \\
&\quad + \frac{2}{\lambda_2 m}\sum_{k\in[m]}\mathbb{E}[L_k(\theta_*) - L_k(\gamma^{t-1}) + \frac{\beta}{2}\|\tilde{\theta}_k^t - \gamma^{t-1}\|^2] \\
&\quad + \frac{2}{\lambda_2 m}\sum_{k\in[m]}\mathbb{E}\left[\left\langle \gamma^{t-1} - \theta_*, -\lambda_1\text{sign}(\tilde{\theta}_k^t - \theta^{t-1})\right\rangle\right] \qquad (33) \\
&= \mathbb{E}\|\gamma^{t-1} - \theta_*\|^2 + \mathbb{E}\|\gamma^t - \gamma^{t-1}\|^2 - \frac{2}{\lambda_2}\mathbb{E}[\mathcal{R}(\gamma^{t-1}) - \mathcal{R}(\theta_*)] + \frac{\beta}{\lambda_2}\epsilon_t \\
&\quad - \frac{2\lambda_1}{\lambda_2 m}\sum_{k\in[m]}\mathbb{E}\left[\left\langle \gamma^{t-1} - \theta_*, \text{sign}(\tilde{\theta}_k^t - \theta^{t-1})\right\rangle\right] \qquad (34) \\
&= \mathbb{E}\|\gamma^{t-1} - \theta_*\|^2 + \mathbb{E}\|\gamma^t - \gamma^{t-1}\|^2 - \frac{2}{\lambda_2}\mathbb{E}[\mathcal{R}(\gamma^{t-1}) - \mathcal{R}(\theta_*)] + \frac{\beta}{\lambda_2}\epsilon_t \\
&\quad - \frac{2\lambda_1}{\lambda_2}\left\langle \gamma^{t-1} - \theta_*, \frac{1}{m}\sum_{k\in[m]}\mathbb{E}[\text{sign}(\tilde{\theta}_k^t - \theta^{t-1})]\right\rangle \qquad (35)
\end{aligned}
$$

where (32) follows from Lemma B.3, (33) follows from (15), and (34) follows from the definitions of $\mathcal{R}(\cdot)$ and ϵ_t. □

Lemma B.5. *Algorithm 3 satisfies*

$$
(1 - 5\frac{\beta^2}{\lambda_2^2})\epsilon_t \leq 10\frac{1}{\lambda_2^2}C_{t-1} + 10\beta\frac{1}{\lambda_2^2}\mathbb{E}[\mathcal{R}(\gamma^{t-1}) - \mathcal{R}(\theta_*)] + \frac{5\lambda_1^2}{\lambda_2^2}d
$$

Proof. Starting from the definitions of ϵ_t and γ^t,

$$
\begin{aligned}
\epsilon_t &= \frac{1}{m} \sum_{k \in [m]} \mathbb{E}\|\tilde{\theta}_k^t - \gamma^{t-1}\|^2 \\
&= \frac{1}{m} \sum_{k \in [m]} \mathbb{E}\|\tilde{\theta}_k^t - \theta^{t-1} - \frac{1}{\lambda_2} h^{t-1}\|^2 \\
&= \frac{1}{\lambda_2^2} \frac{1}{m} \sum_{k \in [m]} \mathbb{E}\|\nabla L_k(\theta_k^{t-1}) - \nabla L_k(\tilde{\theta}_k^t) - \lambda_1 \text{sign}(\theta_k^t - \theta^{t-1}) - h^{t-1}\|^2 \qquad (36) \\
&= \frac{1}{\lambda_2^2} \frac{1}{m} \sum_{k \in [m]} \mathbb{E}\|\nabla L_k(\theta_k^{t-1}) - \nabla L_k(\theta_*) + \nabla L_k(\theta_*) - \nabla L_k(\gamma^{t-1}) \\
&\qquad\qquad + \nabla L_k(\gamma^{t-1}) - \nabla L_k(\tilde{\theta}_k^t) - \lambda_1 \text{sign}(\theta_k^t - \theta^{t-1}) - h^{t-1}\|^2 \\
&\le \frac{5}{\lambda_2^2} \frac{1}{m} \sum_{k \in [m]} \mathbb{E}\|\nabla L_k(\theta_k^{t-1}) - \nabla L_k(\theta_*)\|^2 + \frac{5}{\lambda_2^2} \frac{1}{m} \sum_{k \in [m]} \mathbb{E}\|\nabla L_k(\gamma_k^{t-1}) - \nabla L_k(\theta_*)\|^2 \\
&\quad + \frac{5}{\lambda_2^2} \frac{1}{m} \sum_{k \in [m]} \mathbb{E}\|\nabla L_k(\tilde{\theta}_k^t) - \nabla L_k(\gamma^{t-1})\|^2 + \frac{5}{\lambda_2^2} \mathbb{E}\|\lambda_1 \text{sign}(\theta_k^t - \theta^{t-1})\|^2 + \frac{5}{\lambda_2^2} \mathbb{E}\|h^{t-1}\|^2 \qquad (37) \\
&\le \frac{5}{\lambda_2^2} \frac{1}{m} \sum_{k \in [m]} \mathbb{E}\|\nabla L_k(\theta_k^{t-1}) - \nabla L_k(\theta_*)\|^2 + \frac{5}{\lambda_2^2} \frac{1}{m} \sum_{k \in [m]} \mathbb{E}\|\nabla L_k(\gamma_k^{t-1}) - \nabla L_k(\theta_*)\|^2 \\
&\qquad\qquad + \frac{5}{\lambda_2^2} \frac{1}{m} \sum_{k \in [m]} \mathbb{E}\|\nabla L_k(\tilde{\theta}_k^t) - \nabla L_k(\gamma^{t-1})\|^2 + \frac{5\lambda_1^2}{\lambda_2^2} d + \frac{5}{\lambda_2^2} C_{t-1} \qquad (38) \\
&\le \frac{5}{\lambda_2^2} C_{t-1} + \frac{5}{\lambda_2^2} 2\beta\, \mathbb{E}[\mathcal{R}(\gamma^{t-1}) - \mathcal{R}(\theta_*)] + \frac{5\beta^2}{\lambda_2^2} \frac{1}{m} \sum_{k \in [m]} \mathbb{E}\|\tilde{\theta}_k^t - \gamma^{t-1}\|^2 + \frac{5\lambda_1^2}{\lambda_2^2} d + \frac{5}{\lambda_2^2} C_{t-1} \qquad (39) \\
&= \frac{10}{\lambda_2^2} C_{t-1} + \frac{10\beta}{\lambda_2^2} \mathbb{E}[\mathcal{R}(\gamma^{t-1}) - \mathcal{R}(\theta_*)] + \frac{5\beta^2}{\lambda_2^2} \epsilon_t + \frac{5\lambda_1^2}{\lambda_2^2} d,
\end{aligned}
$$

where (36) follows from (11), (37) follows from the relaxed triangle inequality (17), (38) follows from (27), and (39) follows from the definition of C_t, the smoothness, and (16). The last equality follows from the definition of ϵ_t. □

After multiplying (28) by $\kappa (= 10 \frac{m}{P} \frac{1}{\lambda_2} \frac{\lambda_2 + \beta}{\lambda_2^2 - 25\beta^2})$, we obtain the following theorem by summing (B.4) and scaled version of (29).

Theorem B.6. *Given model parameters at the round* $(t-1)$*, Algorithm 3 satisfies*

$$
\begin{aligned}
\kappa_0 \mathbb{E}[\mathcal{R}(\gamma^{t-1}) - \mathcal{R}(\theta_*)] \le (\mathbb{E}\|\gamma^{t-1} - \theta_*\|^2 + \kappa C_{t-1}) - (\mathbb{E}\|\gamma^t - \theta_*\|^2 + \kappa C_t) + \kappa \frac{P}{2m} \lambda_1^2 \\
- \frac{2\lambda_1}{\lambda_2} \left\langle \gamma^{t-1} - \theta_*, \frac{1}{m} \sum_{k \in [m]} \mathbb{E}[\text{sign}(\tilde{\theta}_k^t - \theta^{t-1})] \right\rangle.
\end{aligned}
$$

where $\kappa = 10 \frac{m}{P} \frac{1}{\lambda_2} \frac{\lambda_2 + \beta}{\lambda_2^2 - 25\beta^2}, \kappa_0 = \frac{2}{\lambda_2} \frac{\lambda_2^2 - 25\lambda_2\beta - 50\beta^2}{\lambda_2^2 - 25\beta^2}$*. Note that the expectations taken above are conditional expectations given model parameters at time* $(t-1)$*.*

Proof. Summing Lemma $B.4$ and κ-scaled version of (28), we have

$$\begin{aligned}
&\mathbb{E}\|\gamma^t - \theta_*\|^2 + \kappa C_t \\
&\leq \mathbb{E}\|\gamma^{t-1} - \theta_*\|^2 + \kappa C_{t-1} - \kappa\frac{P}{m}C_{t-1} + \kappa\frac{2\beta^2 P}{m}\epsilon_t + \kappa\frac{4\beta P}{m}\mathbb{E}[\mathcal{R}(\gamma^{t-1}) - \mathcal{R}(\theta_*)] \\
&- \frac{2}{\lambda_2}\mathbb{E}[\mathcal{R}(\gamma^{t-1}) - \mathcal{R}(\theta_*)] + \frac{\beta}{\lambda_2}\epsilon_t + \mathbb{E}\|\gamma^t - \gamma^{t-1}\|^2 - \frac{2\lambda_1}{\lambda_2 m}(\gamma^{t-1} - \theta_*)\sum_{k\in[m]}\mathbb{E}[\text{sign}(\tilde{\theta}_k^t - \theta^{t-1})].
\end{aligned} \tag{40}$$

As $\mathbb{E}\|\gamma^t - \gamma^{t-1}\|^2 \leq \epsilon_t$ by (29), we have

$$\kappa\frac{2\beta^2 P}{m}\epsilon_t + \frac{\beta}{\lambda_2}\epsilon_t + \mathbb{E}\|\gamma^t - \gamma^{t-1}\|^2 \leq \kappa\frac{2\beta^2 P}{m}\epsilon_t + \frac{\beta}{\lambda_2}\epsilon_t + \epsilon_t. \tag{41}$$

This can be further bounded as follows.

$$\begin{aligned}
(41) &= \left(10\frac{m}{P}\frac{1}{\lambda_2}\frac{\lambda_2+\beta}{\lambda_2^2 - 25\beta^2}\cdot\frac{2\beta^2 P}{m} + \frac{\beta}{\lambda_2} + 1\right)\epsilon_t \\
&= \frac{1}{\lambda_2(\lambda_2^2 - 25\beta^2)}\left(20(\lambda_2+\beta)\beta^2 + \beta(\lambda_2^2 - 25\beta^2) + \lambda_2(\lambda_2^2 - 25\beta^2)\right)\epsilon_t \\
&= \frac{\lambda_2(\lambda_2+\beta)}{\lambda_2^2 - 25\beta^2}\left(1 - 5\frac{\beta^2}{\lambda_2^2}\right)\epsilon_t \\
&\leq \frac{\lambda_2(\lambda_2+\beta)}{\lambda_2^2 - 25\beta^2}\left(\frac{10}{\lambda_2^2}C_{t-1} + \frac{10\beta}{\lambda_2^2}\mathbb{E}[\mathcal{R}(\gamma^{t-1}) - \mathcal{R}(\theta_*)] + \frac{5\lambda_1^2}{\lambda_2^2}d\right) \\
&= \kappa\frac{P}{m}C_{t-1} + \kappa\frac{\beta P}{m}\mathbb{E}[\mathcal{R}(\gamma^{t-1}) - \mathcal{R}(\theta_*)] + \kappa\frac{P}{2m}\lambda_1^2 d,
\end{aligned}$$

where the inequality follows from Lemma B.5. Then, (40) term will be

$$\begin{aligned}
\mathbb{E}\|\gamma^t - \theta_*\|^2 + \kappa C_t \leq \mathbb{E}\|\gamma^{t-1} - \theta_*\|^2 + \kappa C_{t-1} - \kappa_0\mathbb{E}[\mathcal{R}(\gamma^{t-1}) - \mathcal{R}(\theta_*)] + \kappa\frac{P}{2m}\lambda_1^2 d \\
- \frac{2\lambda_1}{\lambda_2}\left\langle\gamma^{t-1} - \theta_*, \frac{1}{m}\sum_{k\in[m]}\mathbb{E}[\text{sign}(\tilde{\theta}_k^t - \theta^{t-1})]\right\rangle.
\end{aligned}$$

Rearranging terms, we prove the claim. □

Now we are ready to prove the main claim by combining all lemmas. Let us take the sum on both sides of Lemma B.6 over $t = 1, \ldots, T$. Then, telescoping gives us

$$\begin{aligned}
\kappa_0\sum_{t=1}^{T}\mathbb{E}[\mathcal{R}(\gamma^{t-1}) - \mathcal{R}(\theta_*)] \leq (\mathbb{E}\|\gamma^0 - \theta_*\|^2 + \kappa C_0) - (\mathbb{E}\|\gamma^T - \theta_*\|^2 + \kappa C_T) + T(\kappa\frac{P}{2m}\lambda_1^2) \\
- \frac{2\lambda_1}{\lambda_2}\sum_{t=1}^{T}\left\langle\gamma^{t-1} - \theta_*, \frac{1}{m}\sum_{k\in[m]}\mathbb{E}[\text{sign}(\tilde{\theta}_k^t - \theta^{t-1})]\right\rangle.
\end{aligned}$$

Since κ is positive if $\lambda_2 > 27\beta$, we can eliminate the negative term in the middle. Then,

$$\begin{aligned}
\kappa_0\sum_{t=1}^{T}\mathbb{E}[\mathcal{R}(\gamma^{t-1}) - \mathcal{R}(\theta_*)] \leq \mathbb{E}\|\gamma^0 - \theta_*\|^2 + \kappa C_0 + T(\kappa\frac{P}{2m}\lambda_1^2 d) \\
- \frac{2\lambda_1}{\lambda_2}\sum_{t=1}^{T}\left\langle\gamma^{t-1} - \theta_*, \frac{1}{m}\sum_{k\in[m]}\mathbb{E}[\text{sign}(\tilde{\theta}_k^t - \theta^{t-1})]\right\rangle.
\end{aligned}$$

Dividing by T and applying Jensen's inequality,

$$\mathbb{E}\left[\mathcal{R}(\frac{1}{T}\sum_{t=0}^{T-1}\gamma^t) - \mathcal{R}(\theta_*)\right] \leq \frac{1}{T}\frac{1}{\kappa_0}(\mathbb{E}\|\gamma^0 - \theta_*\|^2 + \kappa C_0) + \frac{1}{\kappa_0}(\kappa\frac{P}{2m}\lambda_1^2 d) \\ - \frac{1}{T}\frac{2\lambda_1}{\lambda_2}\sum_{t=1}^{T}\left\langle \gamma^{t-1} - \theta_*, \frac{1}{m}\sum_{k\in[m]}\mathbb{E}[\text{sign}(\tilde{\theta}_k^t - \theta^{t-1})]\right\rangle, \tag{42}$$

which completes the proof of Theorem B.1.

B.3 Discussion on Convergence

In this section, we revisit the convergence stated in Theorem 3.1. Recall the bound

$$\mathbb{E}\left[\mathcal{R}\left(\frac{1}{T}\sum_{t=0}^{T-1}\gamma^t\right) - \mathcal{R}(\theta_*)\right] \leq \frac{1}{T}\frac{1}{\kappa_0}(\mathbb{E}\|\gamma^0 - \theta_*\|^2 + \kappa C_0) + \frac{1}{\kappa_0}(\kappa\frac{P}{2m}\lambda_1^2 d) \\ - \frac{1}{T}\frac{2\lambda_1}{\lambda_2}\sum_{t=1}^{T}\left\langle \gamma^{t-1} - \theta_*, \frac{1}{m}\sum_{k\in[m]}\mathbb{E}[\text{sign}(\tilde{\theta}_k^t - \theta^{t-1})]\right\rangle,$$

As we discussed in the main body, the second term is a negligible constant in the range of our hyperparameters as λ_1 is of order of 10^{-4} or 10^{-6}.

Consider the last term where the summand is the inner product between two terms: 1) $\gamma^{t-1} - \theta_*$, the deviation of the averaged local models from the globally optimal model and 2) the average of sign vectors across clients. The deviation term characterizes how much the averaged local models are different from the global model; thus, we can assume that as training proceeds it vanishes or at least is bounded by a constant vector. To argue the average of sign vectors, assume a special case where the sign vectors $\text{sign}(\tilde{\theta}_k^t - \theta^{t-1})$ are IID across clients. To further simplify the argument, let us consider only a single coordinate of the sign vectors, say $X_k = \text{sign}(\tilde{\theta}_k^t(i) - \theta^{t-1}(i))$, and suppose $X_k = \pm 1$ with probability 0.5 each. Then, the concentration inequality (Durrett, 2019) implies that for any $\delta > 0$,

$$\mathbb{P}\left[\frac{1}{m}\sum_{k\in[m]}\text{sign}(\tilde{\theta}_k^t) - \theta^{t-1} > \delta\right] = \mathbb{P}\left[\frac{1}{m}\sum_{k\in[m]}X_k > \delta\right] \leq e^{-\frac{m\delta^2}{2}}$$

holds, which vanishes exponentially fast with the number of clients m. Since m is large in many FL scenarios, the average of sign vectors is negligible with high probability, which in turn implies the last term is also negligible.